

$$\boxed{\frac{\epsilon + P}{\tau} + \frac{d\epsilon}{d\tau} = 0.} \quad (6.34)$$

For $\epsilon(T)$ and $P(T)$, this implies that T is a function of τ , but not of y . This important result originates from the assumption that the proper time τ of a fluid volume element is as given in Eq. (6.26), and it is in particular independent of the transverse coordinates.

For a (nearly) relativistic gas $v_s^2 \lesssim \frac{1}{3}$, and the decrease of the temperature is slow. Explicitly, integrating Eq. (6.20), we obtain, assuming that the velocity of sound changes slowly,

$$T = T_0 \left(\frac{\tau_0}{\tau} \right)^{v_s^2}, \quad (6.35)$$

where the initial temperature T_0 is established at an initial (proper) time τ_0 , at which local thermal equilibrium has been established and the isentropic hydrodynamic expansion begins. In order to decrease the temperature by a factor two, we need the time $\tau \simeq 8\tau_0$.

In a more realistic evolution of a fireball, which allows for transverse expansion, the expansion cooling is faster [58, 163]; see section 6.2. On the other hand, one also must allow for a less than fully relativistic sound velocity. The properties of the equation of state obtained on the lattice suggest that, in the vicinity of the phase transition, i.e., for $T < 2T_c$, there are significant deviations from ideal-gas behavior. A seemingly small change in v_s matters: we note that, when $v_s \simeq 0.5$ (recall that $1/\sqrt{3} \simeq 0.58$), for the scaling solution Eq. (6.35), the time needed to decrease the temperature by a factor of two increases two-fold to $\tau \simeq 16\tau_0$.

7 Entropy and its relevance in heavy-ion collisions

7.1 Entropy and the approach to chemical equilibrium

Entropy is a quantity characterizing the arrow of time in the evolution of a physical system – in every irreversible process the entropy increases. In elementary interactions, and in particular those involving relativistic collisions of two large atomic nuclei, there is considerable production of particles and hence of entropy. A number of questions arise naturally in this context:

1. When and how is entropy produced in a quantum process, such as a nuclear collision?
2. How is production of hadronic particles related to production of entropy?
3. How does one measure the entropy produced in the reaction?

In the deconfined phase the color degree of freedom is ‘melted’. Therefore, the specific entropy content per baryon (S/b), evaluated at some given (measured) values of statistical parameters, is generally greater in the deconfined state than it is in the confined state. Entropy can only increase, and thus, once an entropy-rich state has formed, we have an opportunity, by measurement of the entropy created in the heavy-ion collision, to determine whether the color bonds of valence quarks present in the collision have been broken.

The final entropy content of the hadronic particles emerging has to exceed the initial entropy of the thermal state. In fact, quantitative studies show that very little additional entropy is produced during the entire evolution of a fireball, after the initial thermalization stage. For this reason, the final hadronic state conveys key information about the initial thermal state of dense and hot hadronic matter. For example, in the expanding quark–glue fireball the quasi-entropy-conserving evolution has been confirmed within a model study involving parton cascade [129]. The final-state entropy is largely produced in the first instant of heavy-ion collision.

The entropy can be obtained using the momentum-distribution function $f_{B,F}$:

$$S_{B,F} = \int d^3x \int \frac{d^3p}{(2\pi)^3} [\pm(1 \pm f_{B,F}) \ln(1 \pm f_{B,F}) - f_{B,F} \ln f_{B,F}]. \quad (7.1)$$

The upper sign + is for bosons (B) and the lower sign – is for fermions (F), which is somewhat counterintuitive, but in fact in agreement with Fermi and Bose statistics. We are reminded of this change by the change in the usual sequence of letters ‘F, B’ in the subscript.

There are two well-known ways to obtain Eq. (7.1). It follows (up to normalization) from Boltzmann’s H-function in the study of momentum equilibration. It also arises naturally on rewriting Eq. (10.25) in terms of the single-particle distribution function Eq. (4.42). Since in this approach the statistical definition of entropy, which corresponds to the thermal definition, is used, the normalization is fixed by the laws of thermodynamics.

Entropies of different particles add, and the entropy of particles and antiparticles adds as well. The entropy of fermions, in Eq. (7.1), vanishes in the pure quantum-state limit for $T \rightarrow 0$, since the value of the particle-occupancy probability is either unity or zero. The ‘classical’ Boltzmann limit arises when $f_{B,F} \ll 1$. In this case, with $f_{B,F} \rightarrow f$,

$$S_{cl} \equiv \int d\omega f \ln\left(\frac{e}{f}\right) = \int d\omega (f - f \ln f), \quad \int d\omega \equiv \int d^3x \int \frac{d^3p}{(2\pi)^3}. \quad (7.2)$$

Generally, expression Eq. (7.1) is presented as the generalization of the well-known classical micro-canonical definition Eq. (7.2) to quantum gases; however, this language leads to the (frequent) omission of the first term on the right-hand side, which is the number of particles present, and which comprises 25% of the total entropy of the relativistic gas.

We will study the entropy of a statistical gas in more detail in section 10.6. We note that, for massless particles (quarks, gluons), the entropy per particle following from Eq. (7.1) and Eq. (7.2) is

$$\frac{S}{N} \Big|_{m=0}^{\text{B}} = 3.61, \quad \frac{S}{N} \Big|_{m=0}^{\text{cl}} = 4, \quad \frac{S}{N} \Big|_{m=0}^{\text{F}} = 4.20. \quad (7.3)$$

The effect of the finite pion mass is to increase the entropy per particle, see Eq. (10.79) and Fig. 10.4 on page 206. Each pion (a boson) emerging carries away just about 4 units of entropy from the source as long as the temperature is $T \simeq m_\pi$. These results are for a chemically equilibrated system. In general, below equilibrium at a given fixed temperature, the entropy density is lower, but the entropy per particle is higher than that in Eq. (7.3), and the opposite is true for a system above chemical equilibrium, $\gamma > 1$; section 7.5.

For an isolated system, like our hadronic fireball, a very important physical property is that relatively little entropy is generated in the approach to chemical equilibrium, both from above and from below. This happens since the change in number of particles consumes or releases thermal energy and this changes the temperature. Thus, even after chemical equilibration, the final-state entropy content is closely related to the initial entropy of the thermal state generated in the collision.

To demonstrate this, we obtain the shape of the particle-occupancy probability f of particles in the isolated fireball from the Boltzmann H-theorem result, i.e., the principle that a physical system evolves toward maximum entropy for a given energy and number of particles in the system. We seek to maximize the entropy Eq. (7.1) subject to these constraints, i.e.,

$$T(f) = \int d\omega [\pm(1 \pm f) \ln(1 \pm f) - f \ln f - (\alpha_f + \beta \epsilon_f) f], \quad (7.4)$$

as a functional of the distribution shape $\{f\}$. Here, $d\omega$ is the phase-space integral seen in Eqs. (7.1) and (7.2).

The results are the standard Fermi and Bose distributions Eq. (4.42), including the chemical nonequilibrium factor $\gamma = e^{-\alpha}$ which allows that the particle number is fixed independently from the temperature,

$$f_{\text{F,B}} = \frac{1}{e^{\beta \epsilon + \alpha} \pm 1}. \quad (7.5)$$

This demonstrates that an isolated system in the presence of suitable internal dynamics, e.g., two-body elastic collisions, will evolve toward the kinetic-equilibrium statistical Bose/Fermi distributions, which may be in chemical nonequilibrium expressed by $\gamma \neq 1$, depending on the initial energy and number of particles. When inelastic particle-production processes are occurring, we further expect that also chemical equilibrium should be reached, but on a slower time scale; see section 5.5.

Now, we are ready to show that the entropy content of a chemically not fully equilibrated system is nearly the same as the entropy content of a system in equilibrium. For the Boltzmann approximation, we can show this analytically. The factor γ becomes a normalization factor that describes the average occupancy of the phase space relative to the equilibrium value; the additive term describes how the entropy per particle changes as the occupancy changes. We find in the Boltzmann limit

$$\mathcal{N} = \gamma \mathcal{N}|_{\text{eq}}, \quad (7.6)$$

$$\mathcal{E} = \gamma \mathcal{E}|_{\text{eq}}, \quad (7.7)$$

$$\mathcal{S} = \gamma \mathcal{S}|_{\text{eq}} + \ln(\gamma^{-1}) \gamma \mathcal{N}|_{\text{eq}}. \quad (7.8)$$

For massless particles, the phase-space integrals are easily performed and one obtains, see chapter 4,

$$\mathcal{N}^0 = aV\gamma T^3, \quad (7.9)$$

$$\mathcal{E}^0 = 3aV\gamma T^4, \quad (7.10)$$

$$\mathcal{S}^0 = 4aV\gamma T^3 + \ln(\gamma^{-1}) aV\gamma T^3, \quad (7.11)$$

where $a = g/\pi^2$ and g is the degeneracy. One easily finds how, for $\mathcal{E}^0 = \text{constant}$, the entropy varies as a function of γ ,

$$\mathcal{S} \propto \gamma^{1/4}(4 - \ln \gamma). \quad (7.12)$$

This functional has a very weak maximum at $\gamma = 1$. For example, at $\gamma = 2$ the entropy is 98.3% of the value at $\gamma = 1$.

One could imagine that an important change in number of particles is required when γ increases by say a factor of ten from 0.1 to 1. However, since the total energy and volume of the system (and hence the energy density) do not vary, we obtain a result that contradicts our intuition. Namely, at a high initial temperature the phase space is much greater and, in the Boltzmann approximation, the number of particles scales with γT^3 , Eq. (7.6). Since $\mathcal{E}/V \propto \gamma T^4$, we obtain

$$\mathcal{N}|_{\mathcal{E}/V} \propto \gamma^{1/4}. \quad (7.13)$$

Thus, a ten-fold increase in γ is accompanied by a 1.8-fold increase in number of particles.

At this point, it is perhaps wise to briefly review the more familiar case of a fixed-temperature environment (a heat bath) in order to understand better the difference from the isolated-fireball system. Consider the ‘black-body’ radiator: a thermally insulated box with a small emission hole, for which the loss of energy due to radiation through the hole is externally compensated by keeping the temperature constant: the spectrum of the emitted radiation displays the Planck shape which minimizes the free-energy content \mathcal{F} of the photon gas, at a fixed temperature of the walls – this spectrum is arising from interaction of the photons with the walls, with the spectrum and number of photons changing due to absorption and re-emission by the walls. Recalling now that $\mathcal{F} = \mathcal{E} - TS$, we can combine Eqs. (7.6) and (7.8), which gives, in the Boltzmann limit,

$$\mathcal{F} = -aVT^4\gamma[1 + \ln(\gamma^{-1})], \quad (7.14)$$

with a minimum at $\gamma = 1$. However, now a change by a factor of two in γ , at fixed T , leads to a change by 35% in the value of the free energy and an even greater change in entropy. Clearly, at fixed T , the equilibrium point $\gamma \rightarrow 1$ is much better defined than it is at fixed \mathcal{E} .

The lack of sensitivity of entropy to chemical equilibration for an isolated fireball assures that there is ample room to generate nonequilibrium particle yields during the dynamic evolution of the system. Given that the system we are considering is actually subject to a dynamic evolution, with expanding volume V , it is natural to expect that chemical equilibrium is an exception rather than a rule.

7.2 Entropy in a glue-ball

We are now ready to examine in detail the simplest system of dynamic interest to us. We consider an initially thermal glue-parton ball far from particle-abundance equilibrium. There are glue interactions that are producing particles, driving the system to chemical equilibrium while the temperature decreases, due to sharing of a fixed available amount of thermal energy by an ever larger number of constituents. We assume, in the example below, that, when chemical equilibrium is reached, the glue-gas state is at $T = 250$ MeV.

The intuitive expectation is that a lot of entropy is produced while this system evolves toward the particle-abundance equilibrium. However, this is not so [179]. The reason is that, as the equilibrium in particle-number abundance is approached, we must adjust the temperature of the system. There is a subtle balance between the different effects, and the result is that we find considerable constancy of the entropy of the isolated particle-producing system.

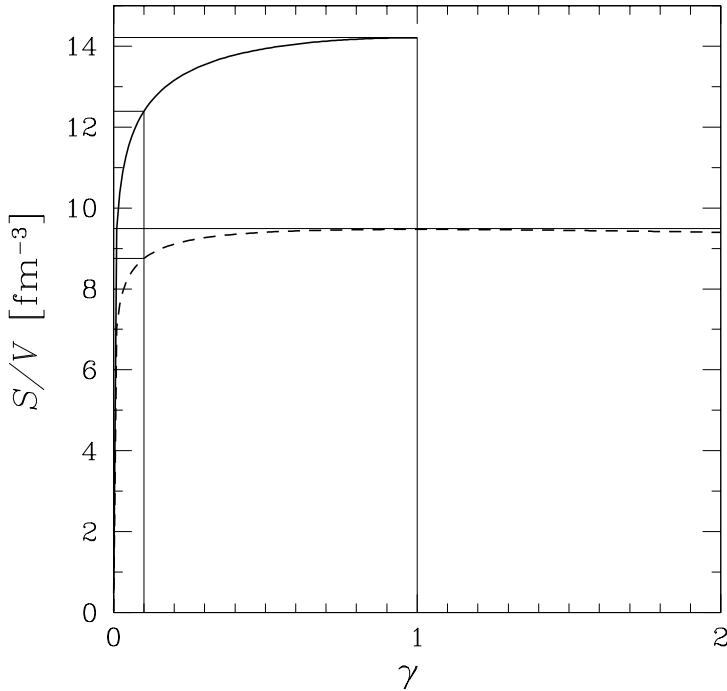


Fig. 7.1. The entropy density S/V (units fm^{-3}), at a fixed energy density $E/V = 2.66 \text{ GeV fm}^{-3}$, for $m_g = 0$ (solid line), and at $E/V = 1.89 \text{ GeV fm}^{-3}$ for $m_g = 0.450 \text{ GeV}$ (dashed line), for a (gluon) Bose gas, as a function of the chemical occupancy γ , with $T(\gamma = 1) = 250 \text{ MeV}$.

We consider both the massless-gluon case and the case of thermally massive gluons, choosing for the thermal gluon mass $m_g^{\text{th}} = 0.450 \text{ GeV}$, see Fig. 16.3 on page 308. A massless-gluon (Bose) gas, with $g = 16$, has an energy density $E/V = 2.66 \text{ GeV fm}^{-3}$, at $T = 250 \text{ MeV}$, at the chemical-equilibrium point $\gamma = 1$. The massive gas, at the chemical-equilibrium point $\gamma = 1$ at $T = 250 \text{ MeV}$, has $E/V = 1.89 \text{ GeV fm}^{-3}$.

In Fig. 7.1, we see the entropy density S/V (units fm^{-3}) as a function of γ ; the solid line is for massless gluons and the dashed line is for massive gluons. The maximum in entropy at $\gamma = 1$ is shallower than would be the case for a Boltzmann gas. The curves end at the singularity of the Bose distribution function, $\gamma = 1$ for massless gluons, and $\gamma_c = e^{m_g/T} \sim 2.7$ (beyond the range shown in Fig. 7.1), which values cannot be exceeded.

The vertical line, to the left in Fig. 7.1, shows that the entropy content of the hot-gluon system at $\gamma = 0.1$ is already nearly 90% of the chemical-equilibrium entropy. The ‘hot’ glue is at this point at $T \simeq 453 \text{ MeV}$ for $m_g = 0$, and at $T = 426 \text{ MeV}$ for $m_g = 0.450 \text{ GeV}$.

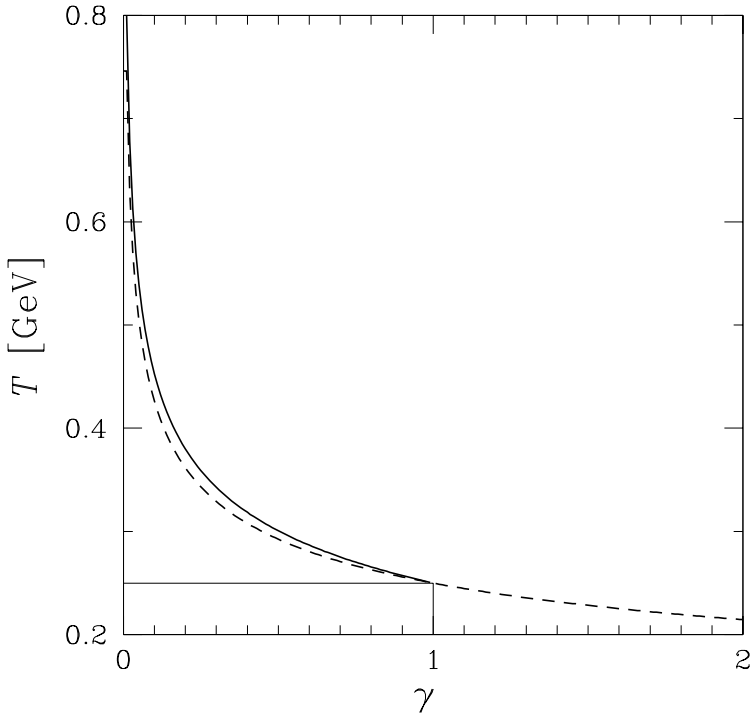


Fig. 7.2. The temperature T as a function of the chemical occupancy γ for massless gluons with $E/V = 2.66 \text{ GeV fm}^{-3}$ (solid line) and $m_g^{\text{th}} = 0.450 \text{ GeV}$, $E/V = 1.89 \text{ GeV fm}^{-3}$ (dashed line). The equilibrium point $\gamma = 1$ has been chosen to occur at $T = 250 \text{ MeV}$.

In order to maintain a fixed value of E/V , the temperature T and phase-space occupancy γ are not independent, and, as a function of γ , the temperature T drops rapidly, which is shown in Fig. 7.2. The dashed line, corresponding to the case of massive gluons, coincides with the solid line (massless gluons) at $\gamma = 1, T = 250 \text{ MeV}$, by token of the judicious choice of E/V . As Fig. 7.2 shows, the temperature can drop rapidly in the process of chemical equilibration of the gluon gas.

It is interesting to note that, when the chemical cooling, seen for small γ in Fig. 7.2, is fastest at small γ , the collective flow of the QGP fireball should not yet be established. Therefore, it is probable that the initial-state cooling is due to chemical processes. The mechanism for a chemical equilibration of the hot initial glue phase which is faster than the volume expansion has been proposed to be inherent in the multi-gluon-production reactions [247], $gg \rightarrow ggg, gggg, \dots$

The number of gluons changes relatively slowly, in particular considering massive (thermal) gluons, as can be seen in Fig. 7.3. In the case of

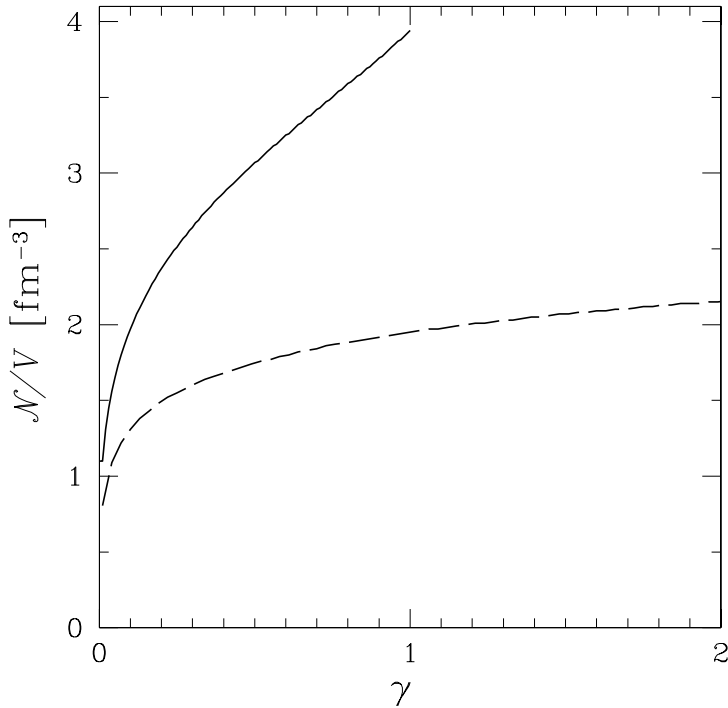


Fig. 7.3. The particle density \mathcal{N}/V (units fm^{-3}) as a function of the chemical occupancy γ . Lines are as in Fig. 7.1.

massless gluons (solid line), when γ increases by a factor of ten from 0.1 to 1, the number of gluons increases five times slower. This increase is considerably more modest for $m_g^{\text{th}} = 0.450$ GeV (dashed line in Fig. 7.3). To understand the greater change seen in Fig. 7.3 compared to Fig. 7.1 it is important to know that the entropy per particle is noticeably greater than four for a system far from chemical equilibrium, Fig. 7.8.

The process of chemical equilibration of glue involves, apart from an increase in the number of gluons, a change in the momentum distribution. In Fig. 7.4, we compare the spectra of gluons initially at $\gamma = 0.1$ with equilibrium $\gamma = 1$. At equilibrium, the temperature is $T = 250$ MeV and we see that the massless- (solid line) and massive-gluon (dashed line) spectra coincide (lines ending at $E \simeq 3.5$ GeV). The ‘missing’ gluons, at low energies, contribute to the difference in energy density (2.66 versus 1.89 GeV fm^{-3} for massless and massive, $m_g = 450$ MeV, gluons, respectively). The relatively slowly falling spectra are for the early hot-glue nonequilibrium stage at $\gamma = 0.1$, at which for massless gluons $T = 453$ MeV and for massive gluons $T = 426$ MeV (values determined for fixed volume and energy of the fireball).

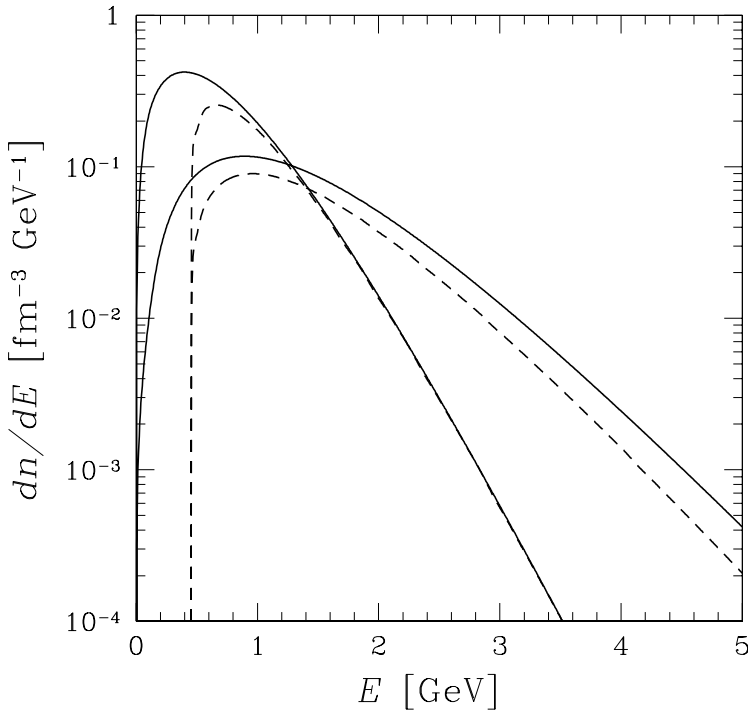


Fig. 7.4. Spectra of massless (solid lines) and $m_g = 450$ MeV (dashed lines), gluons prior to ($\gamma = 0.1$, lines reaching to right lower corner) and at ($\gamma = 1$, $T = 250$ MeV) chemical equilibrium.

We have shown that the dynamics of chemical equilibration is often counterintuitive. In particular, when one is considering the dynamics of an isolated fireball, we learned that the entropy varies little if chemical equilibrium is not maintained. We infer that in a rapid evolution, an isolated system can evolve away from chemical equilibrium, even if this means that the chemical entropy is not at its maximum. On the other hand, since the entropy content is not a sensitive probe of chemical-equilibrium properties we can, in the following study of the experimental entropy production, proceed as if chemical equilibrium were maintained, without loss of generality.

7.3 Measurement of entropy in heavy-ion collisions

The final-state entropy content is visible in the multiplicity of particles produced. In the HG and QGP phases of dense hadronic matter, the entropy content is in general different. The entropy content per participant (specific entropy) offers a method to distinguish these two different

hadronic phases. At a temperature $T > T_c \simeq 160 \text{ MeV}$, the QGP is the phase with the higher specific entropy; this difference occurs because of the liberation of the color degrees of freedom in the color-deconfined QGP phase. The question of whether it is possible to measure the entropy per baryon in the fireball arises. A measure of entropy must count the total production of particles, while the number of participants can be measured using the positive-hadron multiplicity, which comprises, in particular, protons participating in the reaction.

It has been argued that, in the SPS energy range, the ratio of net charge multiplicity to the total charged multiplicity comprises information about the specific entropy content of the matter phase in the fireball [182, 183]:

$$D_Q \equiv \frac{N^+ - N^-}{N^+ + N^-}. \tag{7.15}$$

D_Q is understood to be a function of rapidity when considering particle distribution in rapidity, rather than the total abundance number. In general, D_Q can be measured, it is an easy task if particles are not identified. The sum of positive and negative hadron multiplicity can be identified by the sign of the curvature in a magnetic field, and the emission angle; see Fig. 5.5 and Eq. (5.25).

A first estimate of this ratio is

$$D_Q^{\text{ns}} \approx \frac{A_f}{N_\pi} \frac{0.75}{1 + 0.75(A_f/N_\pi)}, \tag{7.16}$$

where A_f is the number of baryons in the fireball. We have considered only non-strange particles ‘ns’, i.e., pions and nucleons, and assumed that the system is symmetric in isospin, that is half of the participants in the fireball A_f are protons, and all yields of pions are equal: $N_{\pi^+} = N_{\pi^-} = N_{\pi^0} = N_\pi/3$.

As we see in Eq. (7.16), D_Q is indeed a measure of the baryon-to-pion ratio and thus of entropy per participant. However, this estimate Eq. (7.16) is wrong by two partially compensating factors of order 2: both higher-mass non-strange resonances and charged strange particles must also be considered. We recall the significant kaon contribution seen in Eq. (5.33).

Theoretically, such calculations require knowledge of the relative abundances of particles for higher-mass resonances as well as for strange particles. This can be determined in a statistical model of chemical freeze-out as a function of a few parameters, in particular T . Similarly, the entropy per baryon in the fireball is given as a function of the same statistical variables. Both the charge-multiplicity ratio D_Q and the specific entropy S/A_f are known functions of the statistical parameters.

As Eq. (7.16) suggests, the quantity

$$C_Q \equiv D_Q \frac{S}{A_f} \propto D_Q \frac{N_\pi}{A_f} \tag{7.17}$$

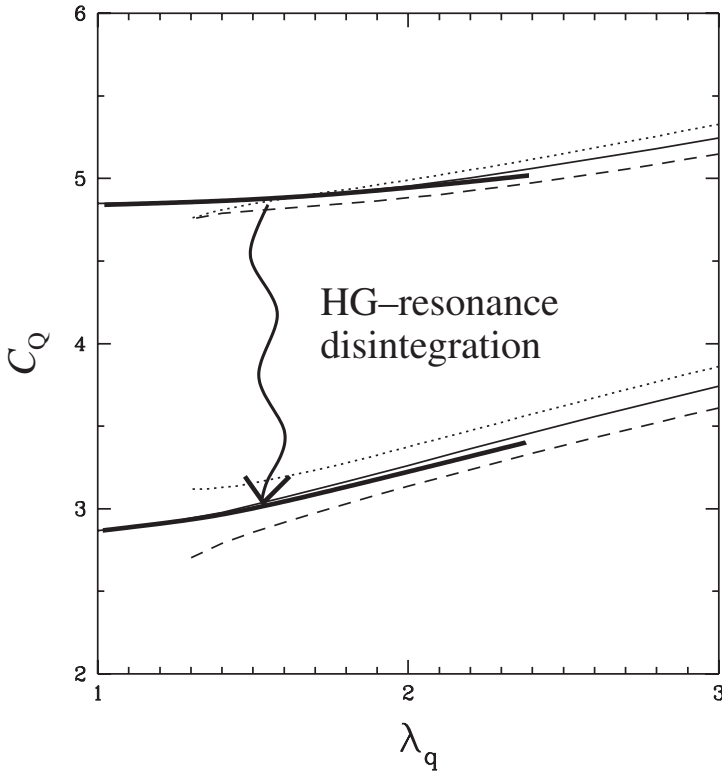


Fig. 7.5. The product $C_Q = D_Q(S/b)$ before (upper curves) and after (lower curves) resonance disintegration, as a function of λ_q , for fixed $\lambda_s = 1 \pm 0.05$ and conserved zero strangeness in an equilibrated HG.

should be a structure constant that depends somewhat on the mixture of hadronic flavors, mass spectrum and similar general hadron-spectrum properties, but should be largely independent from the statistical properties of the system. Once the value of C_Q has been established within a theoretical model, it should then apply in general – a value, $C_Q \simeq 4.5$, was found [182] for a chemically equilibrated system, see the upper line in Fig. 7.5. There is in addition the effect of hadron-resonance decays, and this increases the final-state multiplicity of charged hadrons. According to Eq. (7.15), the value of D_Q diminishes. In consequence, the observable value of $C_Q \simeq 3$ is seen to apply to the lower lines in Fig. 7.5.

7.4 The entropy content in 200A-GeV S–Pb interactions

Since D_Q is generally a small number, it has not been studied extensively. Experiment EMU05 at CERN–SPS has exposed a lead target located in

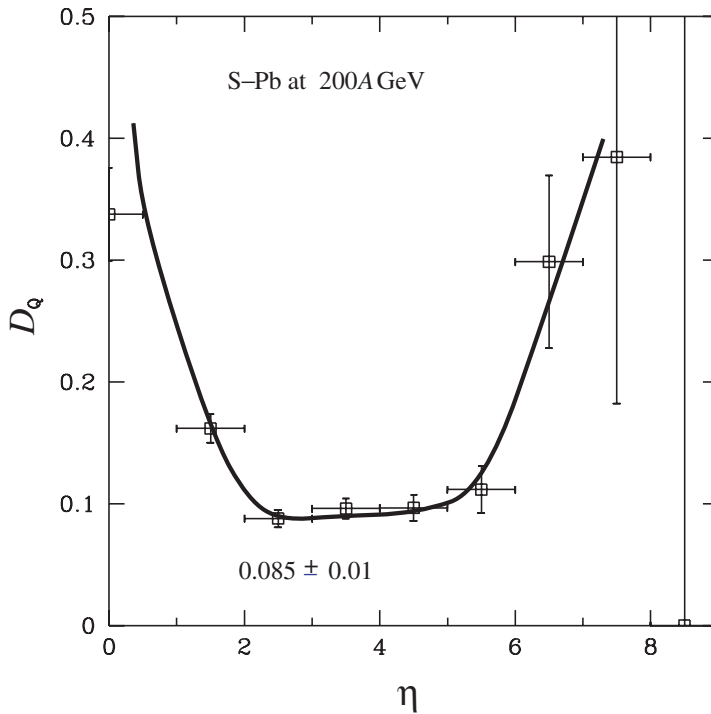


Fig. 7.6. Emulsion data for the charged-particle-multiplicity ratio D_Q obtained in central S–Pb collisions at 200A GeV as a function of pseudorapidity η . The bold black line is drawn to guide the eye.

front of a photographic emulsion to a 200A-GeV beam of sulphur atoms. Since a magnetic field was present, the charge of particles produced was determined and thus the experimental value of D_Q , as a function of pseudorapidity η , could be determined by evaluation of the angle of emission of charged hadrons from the interaction vertex, which fixes η , see Eq. (5.25), and the polarity of charged particles.

Selecting the most central events with charge multiplicity $N^+ + N^- > 300$, corresponding to a total central hadron multiplicity in the range 450–1000, in the central (pseudo)rapidity region, the value

$$D_Q = 0.088 \pm 0.007, \quad \eta \simeq 2.5 \pm 0.5,$$

is found [104, 117]. The distribution $D_Q(\eta)$ is shown in Fig. 7.6. The pseudorapidity distribution is flat in the central region, $\Delta\eta = (\eta - 2.6) \pm 1.5$. This suggests partial transparency and the presence of longitudinal flow in the rapidity distributions of protons and K^+ ; see section 8.3.

Inspecting Fig. 7.5 and Fig. 7.6 we arrive at a first estimate of the entropy content of a fireball formed in these interactions:

$$\frac{S}{b} = \frac{3 \pm 0.1}{0.088 \pm 0.007} = 34 \pm 4.$$

The sources of systematic error involved in the use of D_Q to fix the entropy include the difference in the distribution between rapidity and pseudorapidity, and the uncertainty about yields of strange charged hadrons, which vary with the degree of chemical equilibration of strangeness.

This high value of specific-entropy content in highly central S–Pb 200A-GeV interactions, 40% higher than expected, suggests that an entropy-rich (deconfined) state has been created [182]. Since a high specific-entropy content can be found in the HG phase at smaller values of λ_q , i.e., smaller baryon density, it is important in comparison to the HG to have a good understanding of the baryochemical potential. The value of $\mu_b = 3\mu_q$, see Eq. (4.18), needs to be reduced by nearly a factor of two, to about $\mu_b = 100\text{--}120$ MeV, before the entropy content of HG becomes consistent with these experimental data. Such a small baryochemical potential is not in agreement with many measured yields of hadrons [176]. As this simple case shows it is the simultaneous consideration of several observables (charged-particle asymmetry combined with specific (strange) particle ratios) which allows understanding of the physics of heavy-ion collisions.

7.5 Supersaturated pion gas

The excess of hadron multiplicity (entropy) is a consistently observed phenomenon: the data obtained for Pb–Pb collisions supports this strongly. We have seen in Fig. 1.6 a significant excess of hadron multiplicity in high-energy A–A reactions compared to p–p and low-energy A–A reactions. An important question is how this excess of abundance can be theoretically described in terms of the final-state hadron phase space.

During hadronization, hadrons need to acquire the excess entropy arising from broken color bonds of QGP. We now look for the most entropy-rich hadron gas and consider the super-saturated massive (pion) Bose gas, in which the chemical potential, i.e., the abundance fugacity γ , is nearly compensating for the suppressing effect of the mass, which occurs at $\gamma e^{-m/T} \rightarrow 1$.

For pions, composed of a light-quark–antiquark pair, it is convenient to use as the abundance fugacity

$$\gamma_\pi = \gamma_q^2. \tag{7.18}$$

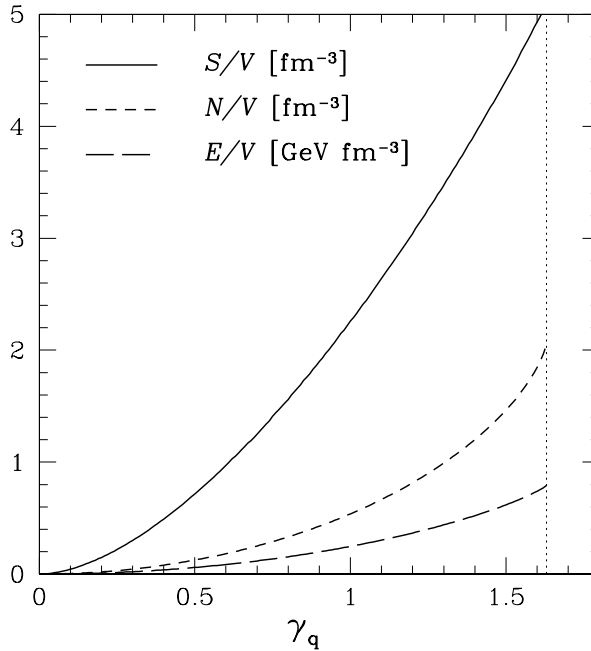


Fig. 7.7. Pion-gas properties N/V for particles, E/V for energy, and S/V for entropy density, as functions of γ_q at $T = 142$ MeV.

This allows one to express, in terms of the abundance of pions, the relation to the abundance of quarks at hadronization, see chapter 19. We study the momentum-space distribution for pions of the form

$$f_{\pi}(E) = \frac{1}{\gamma_q^{-2} e^{E\pi/T} - 1}, \quad E_{\pi} = \sqrt{m_{\pi}^2 + p^2}. \quad (7.19)$$

The range of values for γ_q is bounded from above by the Bose singularity γ_q^c :

$$\gamma_q < \gamma_q^c = e^{m_{\pi}/(2T)}. \quad (7.20)$$

For $\gamma_q \rightarrow \gamma_q^c$, we encounter condensation of pions, the lowest-energy state will acquire macroscopic occupation. Formation of such a condensate ‘consumes’ energy without consuming entropy of the primordial high-entropy QGP phase, and thus is not likely to occur.

In Fig. 7.7, we show the physical properties of a pion gas as functions of γ_q , for a gas temperature $T = 142$ MeV [181]. We see (solid line) that a large range of entropy density can be accommodated by varying the parameter γ_q . A super-saturated pion gas has an entropy density rivaling that of the QGP at the point of transformation into hadrons, as we see on comparing it with Fig. 16.7 on page 315, for $T = 140$ – 160 MeV.

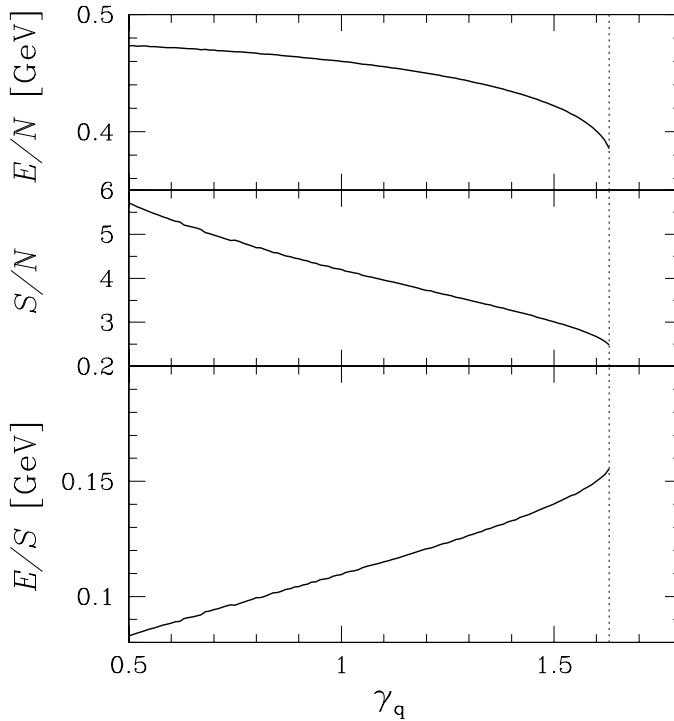


Fig. 7.8. Specific pion-gas properties E/N for energy, S/N for entropy per particle, and E/S for energy per unit of entropy, as functions of γ_q at $T = 142$ MeV.

The presence of chemical nonequilibrium reduces and potentially eliminates discontinuities at the phase transition, promulgating rapid evolution. This implies that, in particular, the sudden hadronization of an entropy-rich QGP should lead to the limiting value $\gamma_q \rightarrow \gamma_q^c$, since other ways of increasing the entropy content involve secondary processes with relatively slow dynamics amongst hadron degrees of freedom. In fact, in an adiabatic equilibrium transformation, one allows an increase in VT^3 , characterizing the entropy content, either by expanding the volume V , or invoking a rise of T (reheating), or both. Another remarkable feature of the chemical-nonequilibrium mechanism is that a first order phase transition may appear in other observables more like a phase transformation without large fluctuations.

It is important to remember that, in the hadronization of a quark–gluon phase, it is relatively easy to ‘consume’ excess energy density, simply by producing a few extra heavy hadrons. However, such particles, being in fact non-relativistic at the temperature considered, are not effective con-

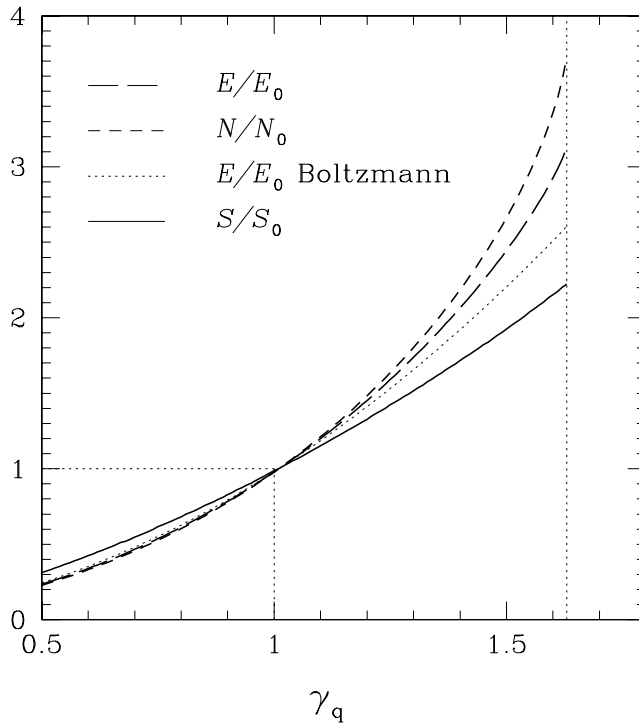


Fig. 7.9. Pion-gas properties (N , number of particles; E , energy; and S , entropy) relative to chemical equilibrium as functions of γ_q for $T = 142$ MeV.

tributors to pressure and entropy. As we see now, the super-saturated pion gas is just the missing element needed in order to allow rapid hadronization.

The specific properties (E/N , S/N , and E/S) of the pion gas are shown in Fig. 7.8, as functions of γ_q . We see a monotonic decrease of energy and entropy per particle while the energy per unit of entropy increases reaching the condition $E/S > T$, which plays an important role in section 19.1. We see that the entropy per pion drops as γ_q increases, and, at the condensation point $\gamma_q \rightarrow \gamma_q^c$, we can add pions without an increase in entropy. Figure 7.8 can be better understood by considering the relative (to chemical equilibrium) physical properties shown in Fig. 7.9. There is, in particular, a large growth in the number of pions, which yield is enhanced at fixed temperature by a factor 3.6 at the condensation point – it is this feature that allows one to hadronize the QGP into a super-saturated pion gas at low, supercooled temperature, accompanied by the experimentally observed excess of pions. We also see, using the energy as an example, that the Boltzmann approximation, i.e., simply a yield factor

γ_q^2 is not producing qualitatively wrong results, even though the increase in number of particles is underestimated by 50%.

7.6 Entropy in a longitudinally scaling solution

We now study the relationship between hadron multiplicity and initial conditions reached for the case of very-high-energy collisions, for which the scaling hydrodynamic solutions can be used to understand the flow of matter. The hydrodynamic expansion of an ideal fluid is entropy-conserving, Eq. (6.13). What this means, in case of the longitudinal expansion, is best seen by considering, in Eq. (6.3), the entropy current $\sigma_\mu = \sigma u_\mu$, and using Eq. (6.32) and the Euler relation Eq. (6.4):

$$0 = \frac{\partial \sigma_\mu}{\partial x_\mu} = \frac{\sigma}{\tau} + \frac{d\sigma}{d\tau} = \frac{1}{\tau} \frac{d(\tau\sigma)}{d\tau}. \quad (7.21)$$

We have

$$\tau\sigma(\tau) = \sigma(\tau_0)\tau_0 = \sigma(\tau_f)\tau_f = \text{constant}, \quad (7.22)$$

where $\tau\sigma$ is a constant of evolution independent of rapidity y .

The physical meaning of conservation of entropy, and thus conservation of $\tau\sigma(\tau)$, becomes clear on remembering the volume element Eq. (6.30). In the locally at rest frame of the fluid (the comoving frame) we have

$$\Delta S = \sigma dz dt = \sigma\tau dy d\tau, \quad (7.23)$$

whence,

$$\boxed{\frac{d}{d\tau} \left(\frac{dS}{dy} \right) = \frac{d}{d\tau} (\tau\sigma) = 0, \quad \frac{dS}{dy} = \text{constant},} \quad (7.24)$$

where, in the last equality, we have used the result Eq. (7.22). dS/dy is independent of y and not a function of τ , i.e., it is independent of the freeze-out condition.

Since entropy is characteristic of the particle yield, Eq. (7.24) implies that the particle multiplicity is flat in rapidity, and is not evolving, i.e., it will not depend on the (uncertain) freeze-out condition. It is established during the initial period of time when the entropy density is built up as the system approaches local thermal equilibrium. Qualitatively, this result is shown in Fig. 5.2; baryons punch through and in between there is a flat distribution in y of particle abundance, since the entropy density per unit rapidity is constant.

It is important to appreciate that, as a matter of principle, the initial entropy density reached in A–A collisions remains naturally undetermined, it arises from microscopic-entropy-producing reactions occurring prior to

the onset of the entropy-conserving hydrodynamic expansion. One can try (and the diverse codes we described in section 6.1 do this) to model the A–A collisions on the basis of the behavior of p–p reactions, but it is far from certain that such an approach will be successful. In other words, we cannot use scaling arguments, Eq. (7.24), to understand how big a value of particle rapidity density we can expect to find. The microscopic physics we introduce explicitly (or sometimes implicitly) into the dynamic model determines the final-state particle multiplicity.

We now relate the observed final-state particle multiplicity to the initial entropy density. Employing the volume element shown in Eq. (7.23), and using the conservation law Eq. (7.24), we obtain

$$\sigma_0 \equiv \frac{dS_0}{dV_0} = \frac{1}{F_\perp} \frac{1}{\tau_0} \frac{dS_0}{dy_0} = \frac{1}{F_\perp \tau_0} \left. \frac{dS}{dy} \right|_f. \quad (7.25)$$

The transverse surface is

$$F_\perp = \pi(1.2 \text{ fm})^2 A^{2/3}, \quad (7.26)$$

as given by the geometry of the collision, at zero impact parameter.

From Eq. (7.25), we obtain, for the initial-state entropy density,

$$\sigma_0 = \frac{1}{\pi(1.2 \text{ fm})^2 A^{2/3} \tau_0} 4 \frac{3}{2} \frac{dN_{\text{ch}}}{dy}, \quad (7.27)$$

where we have assumed that a final-state particle consumes on average 4 units of entropy (see Fig. 10.5), and that the charged-particle multiplicity is two thirds of the total.